

Article

A Modified Marx Generator Circuit with Enhanced Tradeoff between Voltage and Pulse Width for Electroporation Applications

Selvakumar Ganesan ¹, Debarshi Ghosh ¹, Ashu Taneja ^{1,*}, Nitin Saluja ¹, Shalli Rani ^{1,*}, Aman Singh ^{2,3}, Dalia H. Elkamchouchi ⁴ and Irene Delgado Noya ^{2,3}

- ¹ Chitkara University Institute of Engineering and Technology, Chitkara University, Rajpura 140401, India; gselvak@yahoo.com (S.G.); debarshi.ghosh@chitkara.edu.in (D.G.); nitin.saluja@chitkara.edu.in (N.S.)
² Higher Polytechnic School, Universidad Europea del Atlántico, C/Isabel Torres 21, 39011 Santander, Spain; amansingh.x@gmail.com (A.S.); irene.delgado@uneatlantico.es (I.D.N.)
³ Department of Project Management, Universidad Internacional Iberoamericana, Campeche C.P. 24560, Mexico
⁴ Department of Information Technology, College of Computer and Information Sciences, Princess Nourah bint Abdulrahman University, P.O. Box 84428, Riyadh 11671, Saudi Arabia; dhelkamchouchi@pnu.edu.sa
* Correspondence: ashu.taneja@chitkarauniversity.edu.in (A.T.); shalli.rani@chitkara.edu.in (S.R.)

Abstract: Electroporation is a next generation bioelectronics device. The emerging application of electroporation requires high voltage pulses having a pulse-width in the nanosecond range. The essential use of a capacitor results in an increase in the size of the electroporator circuit. This paper discusses the modification of a conventional Marx generator circuit to achieve the high voltage electroporation pulses with a minimal chip size of the circuit. The reduced capacitors are attributed to a reduction in the number of stages used to achieve the required voltage boost. The paper proposes the improved isolation between two capacitors with the usage of optocouplers. Parametric analysis is presented to define the tuneable range of the electroporator circuit. The output voltage of 49.4 V is achieved using the proposed 5-stage MOSFET circuit with an input voltage of 12 V.

Keywords: electroporator; pulse generator; rectangular pulse generator; load independent electroporator



Citation: Ganesan, S.; Ghosh, D.; Taneja, A.; Saluja, N.; Rani, S.; Singh, A.; Elkamchouchi, D.H.; Noya, I.D. A Modified Marx Generator Circuit with Enhanced Tradeoff between Voltage and Pulse Width for Electroporation Applications. *Electronics* **2022**, *11*, 2013. <https://doi.org/10.3390/electronics11132013>

Academic Editor: Davide De Caro

Received: 20 May 2022

Accepted: 24 June 2022

Published: 27 June 2022

Publisher's Note: MDPI stays neutral with regard to jurisdictional claims in published maps and institutional affiliations.



Copyright: © 2022 by the authors. Licensee MDPI, Basel, Switzerland. This article is an open access article distributed under the terms and conditions of the Creative Commons Attribution (CC BY) license (<https://creativecommons.org/licenses/by/4.0/>).

1. Introduction

The technique of applying high voltage electric pulses to tissues or cells to increase their membrane permeability is known as electroporation [1]. The electroporation phenomenon can be understood with the transient pore phenomenon [2]. Electroporation is divided into two categories: reversible electroporation and irreversible electroporation [3]. In reversible electroporation, aqueous pores in the lipid bilayer are created for a very short duration when a high amplitude pulsed electric field is applied, as shown in Figure 1A. These pores disappear when the pulsed electric field is zero. This technique of electroporation is used to allow the entry of molecules, drugs, and other chemicals into the cell. In the irreversible electroporation technique, pores are created in the lipid bilayer upon the application of a pulsed electric field of a long duration, causing cell death as shown in Figure 1B. This technique is used for tissue ablation [4].

Electroporation has been useful in various fields such as biotechnology, medicine, genetics, drug kinetics, and dynamics [3,5–8]. The electroporator creates pores if the pulse voltage is within a precise range [9] and faces a challenge in the application of a high voltage for a short duration of time (milliseconds to nanoseconds). The high pulse period causes cell death; hence, it is dangerous. Modern applications seek to control the pulse period. The biomedical applications of electroporation require the high operational reliability of the instrument.

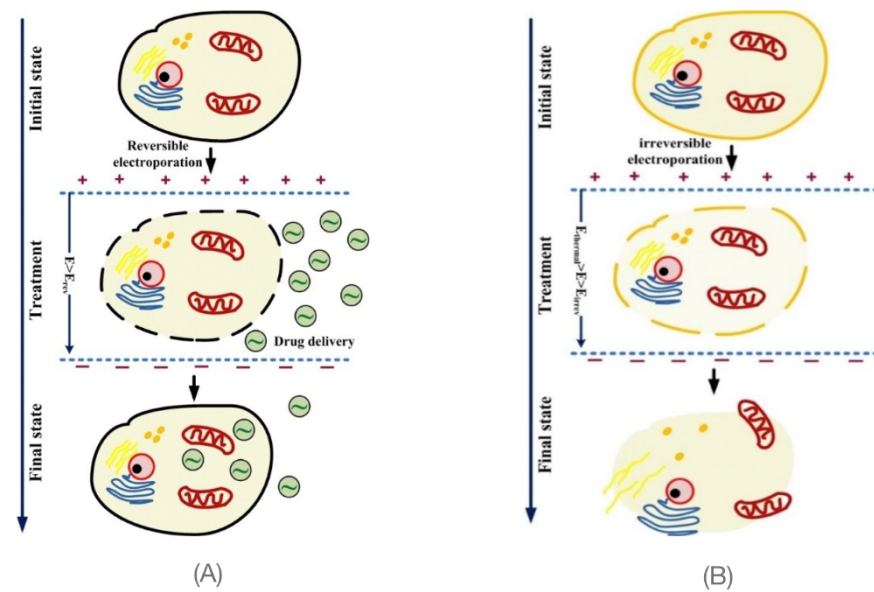


Figure 1. (A) Reversible electroporation process (Chen et al., 2007 [10]), (B) Irreversible electroporation process (Kee et al., 2011 [11]).

Therefore, electroporation depends on the variation of the electric field magnitude in nearby regions. In general, the process of electroporation largely depends on the performance of the electroporator parameters [12]. The important parameters are a precise pulse period and reduced transient time of the pulses [13–15]. In order to produce electroporation pulses, there must be a high voltage, so that it can be controlled in the right way. These high voltage-controlled pulses are then applied to the cell under consideration. There can be a variety of pulses that can be generated as per the specific applications; however, there are two things common to all the pulses. Firstly, the voltages of all the pulses are in the range of 1–100 kV; secondly, the pulse duration ranges from milliseconds to nanoseconds [16]. For high voltage pulses, the duration of the pulse is shorter. Thus, the scope of the pulses that can be used are rectangular, exponential, and a combination of wide and narrow pulses, as illustrated in Figure 2.

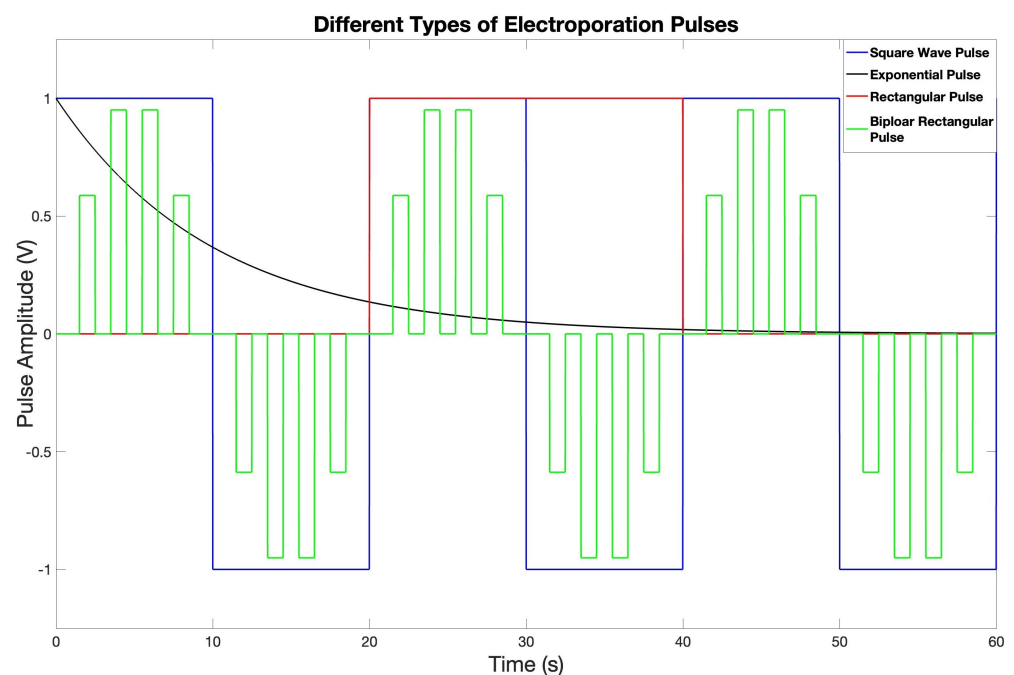


Figure 2. Different type of electroporator waveforms [17].

There are existing circuit topologies that generate high voltage pulses. Examples of such circuits are Marx generators [18–20], diode open switches [21–23], Blumlein generators [21,24,25], and cascaded multilevel invertors [26].

The circuit components are a transistor and a capacitor. The charging and discharging time of the capacitor is an important parameter and defines the tradeoff between the voltage levels and the pulse period [27]. The two main categories of pulse generation are classical pulse generator and power electronics-based pulse generators, as shown in Figure 3.

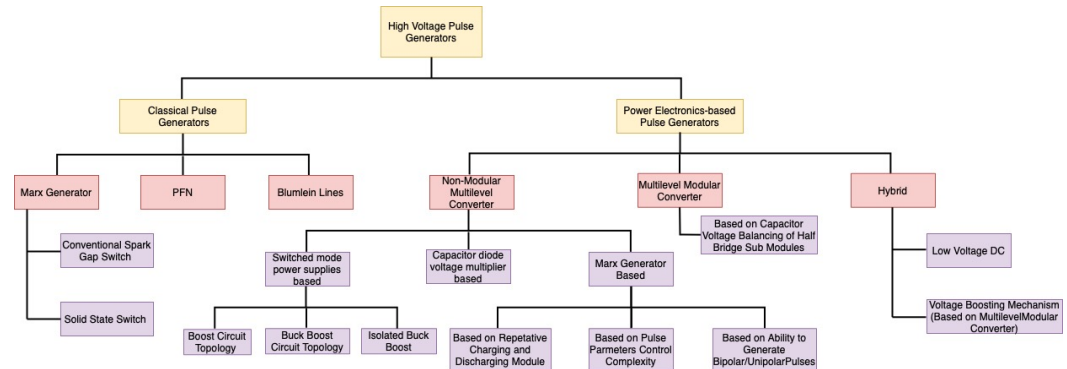


Figure 3. Classification of High Voltage Pulse Generators [28].

The main classical pulse generator is a Marx-based pulse generator. The pulse period ranges from milliseconds to nanoseconds. Generally, the most common way to generate pulses is by using a pulse forming line. The major limitation of this technique is that the pulse duration is fixed by the length of the line. To overcome this drawback, the following techniques can be used:

1. Two Switch Pulse Generator [24]: It is based on two switches whose turn on time is controlled accurately. The duration of the pulse is determined by the delay between the switches.
2. Linear Transformer Driver [29]: Here, magnetic fluxes generated from the discharge circuit are fed to a coaxial cable, so that the voltage is stacked up. By the changing the flux duration, we can vary the pulse properties.
3. Marx Generator [30]: It is a widely used high voltage multiplier for fixed duration pulses. Recently, the spark gaps have been replaced by solid state switches, so that the pulse duration can be adjusted flexibly. In the lower voltage range (<10 kV), solid state switches are the top choice for hard switching, as they can be turned on and switched off, allowing for precise control of the pulse duration.

The Marx-based pulse generator is widely studied and used in different applications of electroporation. A Marx pulse generator generally consists of capacitors, which are charged using an input supply voltage V_s . It also consists of resistors R_c for charging the capacitors, as shown in Figure 4. It is essential to understand that the main control element of the Marx generators is the resistance, which charges the capacitors. The value of the resistors depends on the desired frequency of the pulses.

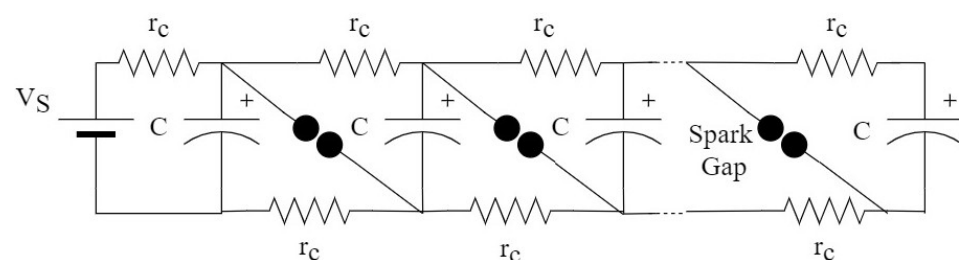


Figure 4. Conventional Marx Generator.

The circuit in Figure 4 consists of spark gaps. The spark gaps act as a switch, and it has the characteristics of a high break voltage in a range up to 30 kV [31]. When the spark gap switches to breakdown, it results in the pulse voltage as output. The process results in enabling all the capacitors in the series. The breakdown of the first spark gap is initiated intentionally, which results in the accumulation of high voltage ($2V_s$) across the second spark gap, and the process continues until all the spark gaps break down. This results in the generation of a pulse of voltage N times the value of the applied voltage V_s across the load.

The conventional Marx generator has two major disadvantages. The first disadvantage is that the Marx generator generates unipolar pulses [31]. The second disadvantage is the size and cost of a Marx generator [32].

The first disadvantage is that the conventional Marx generators are known to generate unipolar pulsating voltages. However, the generation of a bipolar pulse requires the modification in Marx generator. In addition to the conventional circuit fed by positive V_s , an additional circuit with negative input voltage ($-V_s$) needs to be applied. The output of both the Marx generators ($+V_s$ and $-V_s$ input circuits) are connected in a way such that the outputs become differential to each other [31]. The second disadvantage of a conventional Marx generator having a large size and high cost is attributed to the spark gaps. The research has led to the replacement of the spark gaps with solid state switches, such as power transistors. The power transistors offer the additional advantage of the flexibility to tune the pulse width. The solid-state switch also offers the advantages of a lower pulse width, rise time, and fall time, hence improving the pulse shape as per the requirement in an electroporator [32].

The variants of a solid state Marx generator (SSMG) have been proposed and discussed in number of research papers [33,34]. The basic principle of all the variants of SSMGs is similar, but the different variants deploy different circuit topologies. The different topologies vary in their components, such as the capacitors. The different topologies are known to generate either unipolar or bipolar pulses. The limitations of the existing topologies are the lack of modularity, limited pulse repetition range, larger circuits, and improper pulse shapes [28].

A detailed comparison of the present state-of-the-art for electroporator circuits is presented in Table 1.

Table 1. Comparison of the present state-of-the-art for electroporator circuits.

Ref No.	Technology Used	Quantitative Analysis	Advantage	Limitation
[35]	GaN	Frequency: 1 MHz Output Voltage: 2000 V	Advanced use for cancer treatments	Circuit is limited to sinusoidal waveforms, adaptation of resonant tank including frequency resolution is required
[36]	Multilevel Converter	Frequency: 10 KHz Output Voltage: 500 V	Step-up power electronic converter topology for generating the required HV pulses from a relatively low input voltage	This topology can only generate pulses in the KHz range.
[37]	SEPIC	Frequency: 50 KHz Output Voltage: 10 kV	Discontinuous conduction mode operation with continuous input current. Its fewer components is an added advantage	It can only generate pulses in the KHz range

Table 1. Cont.

Ref No.	Technology Used	Quantitative Analysis	Advantage	Limitation
[38]	MOSFET	Frequency: 50 Hz Output Voltage: 1 kV	MOSFETs are advantageous for the usage of a well-controlled electromanipulation technique, cost effective	Not suitable for high frequency range
[39]	SiC-MOSFET	Frequency: 10 Hz Output Voltage: 2 KV	Rectangular output pulse with a controllable amplitude, pulse width and repetition rate, a high voltage gain	Higher parasitic capacitance reduces the speed
[40]	MOSFET	Frequency: 10 Hz Output Voltage: 3 kV	This circuit is designed to be independent of the buffer bioimpedance	Wider range of frequencies is limited
[41]	MOSFET	Frequency: 4 MHz Output Voltage: 1 kV	Control module, a pulse generation circuit, and a high voltage switch using a power MOSFET	Peak transfection rate is only 48%
[42]	MOSFET	Frequency: 500 KHz Output Voltage: 1 kV	It produces high-frequency bipolar high voltage pulse bursts on resistive-type loads, intended for medical applications. Used for tumor treatment	Not suitable for high frequency range
[43]	Flyback Converter	Frequency: 100 KHz Output Voltage: 50 kV	Smaller space, low cost	The oscillator reaches 100 kHz, and the maximum voltage V_{max} pulse is approximately 52.5 kV
[44]	MOSFET	Frequency: 20 KHz Output Voltage: 1 kV	Cascaded Boost Converter topology	Well-synchronized driver circuit needed to trigger individual MOSFETs

This paper presents a modified Marx generator, which addresses the challenges discussed above, such as a bipolar pulse generation with the desired pulse shape properties, in addition to the optimized size and cost of the circuit. The circuit design proposed in this paper achieves the bipolar shape without utilizing the two Marx circuits, hence optimizing the size and cost of the circuit. Further, the flexibility in the range of pulse repetition frequency is achieved with the usage of power MOSFETs. The MOSFET IXTF 1N400 is used as the switching element in the simulation of the proposed Marx Generator. The MOSFET supports a high V_{DSS} up to 4000 V and a rise time and fall time of 24 and 90 ns, respectively. The MOSFET has a nanosecond range slew rate as reported in the literature. Further, the pulse shapes are optimized by reducing the dependency of the output wave on the roll-off properties of the capacitors in the circuit. The modified Marx generator proposed in the circuit exploits the improved isolation between two parallel capacitors of the circuit with the usage of optocouplers [45]. The switching of MOSFETs is controlled by the optocoupler, which also determines the frequency of the high voltage pulses. The values of the components of the circuit are calculated in Section 2. The circuit is analysed with a simulation of the proposed circuit topology. The parametric analysis is presented

The simulation was performed in Proteus simulation software, which is a circuit simulator with the definition of the components added into the customized library, as shown in Figure 4. The input of the circuit was 12 V DC, and the optocoupler was used for switching the MOSFET. The circuit generated pulses of 1 ns. The requirement was to generate the rectangular pulses with the ON time less than the OFF time. Two circuits are presented in this paper for a modified Marx generator. Figure 6 shows the modified Marx generator without an optocoupler, and Figure 7 shows the modified Marx generator with an optocoupler. The two circuits were designed to analyse the significance of optocoupler in the circuit.

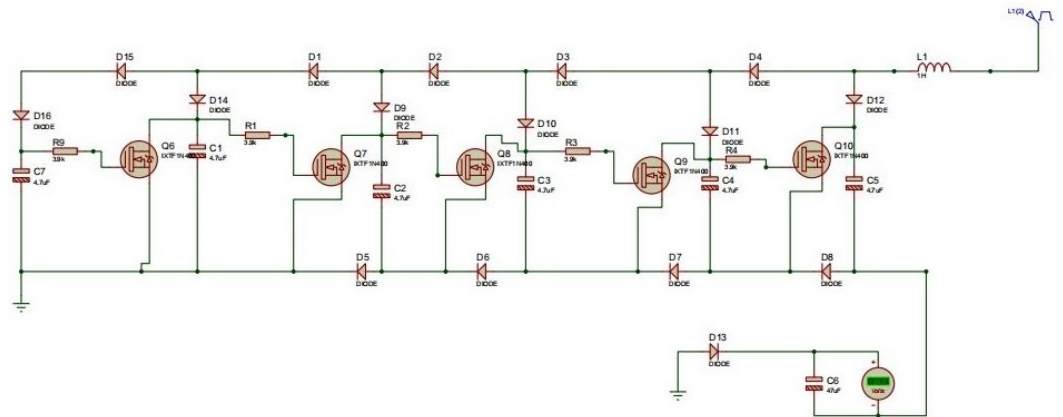


Figure 6. Multistage modified Marx generator without an optocoupler.

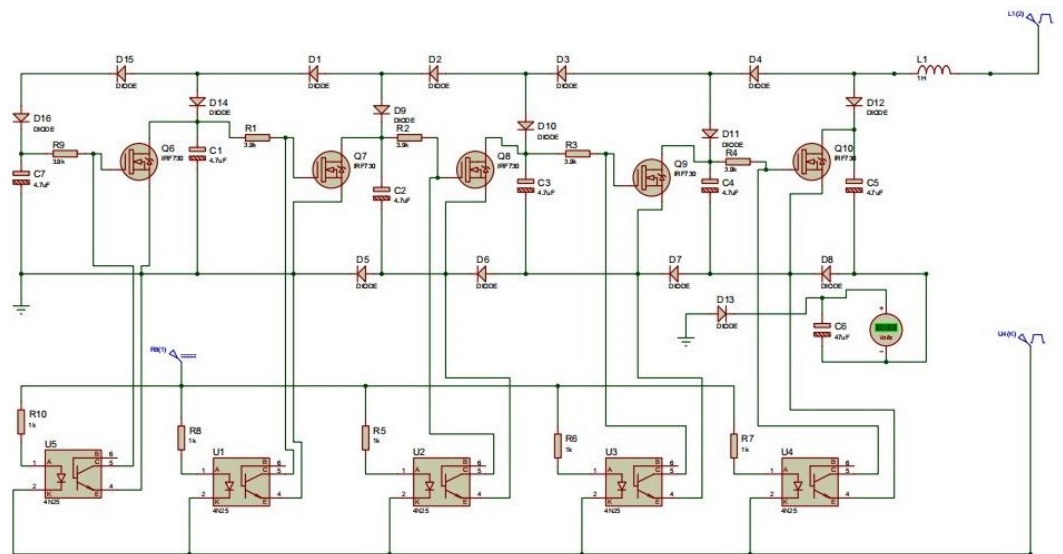


Figure 7. Circuit diagram of the modified Marx pulse generator circuit with an optocoupler.

3. Results and Discussion

The simulated multistage (5-stage) modified Marx generator circuit produced an output pulse of 49 V from the input 12 V DC. The pulse produced was a rectangular pulse suitable for electroporation application, as shown in Figure 7. The voltage multiplication factor depended upon the number of stages used in the Marx generator. Here, a four-stage Marx generator was used, so the output was four times the input voltage. The capacitance values were varied, and the calculated value of the capacitance, which was 4.7 nF, produced the maximum voltage and had a rise time of 4.6 ns. The pulses generated in the circuit were bipolar, as shown in Figure 8.

DSO Output

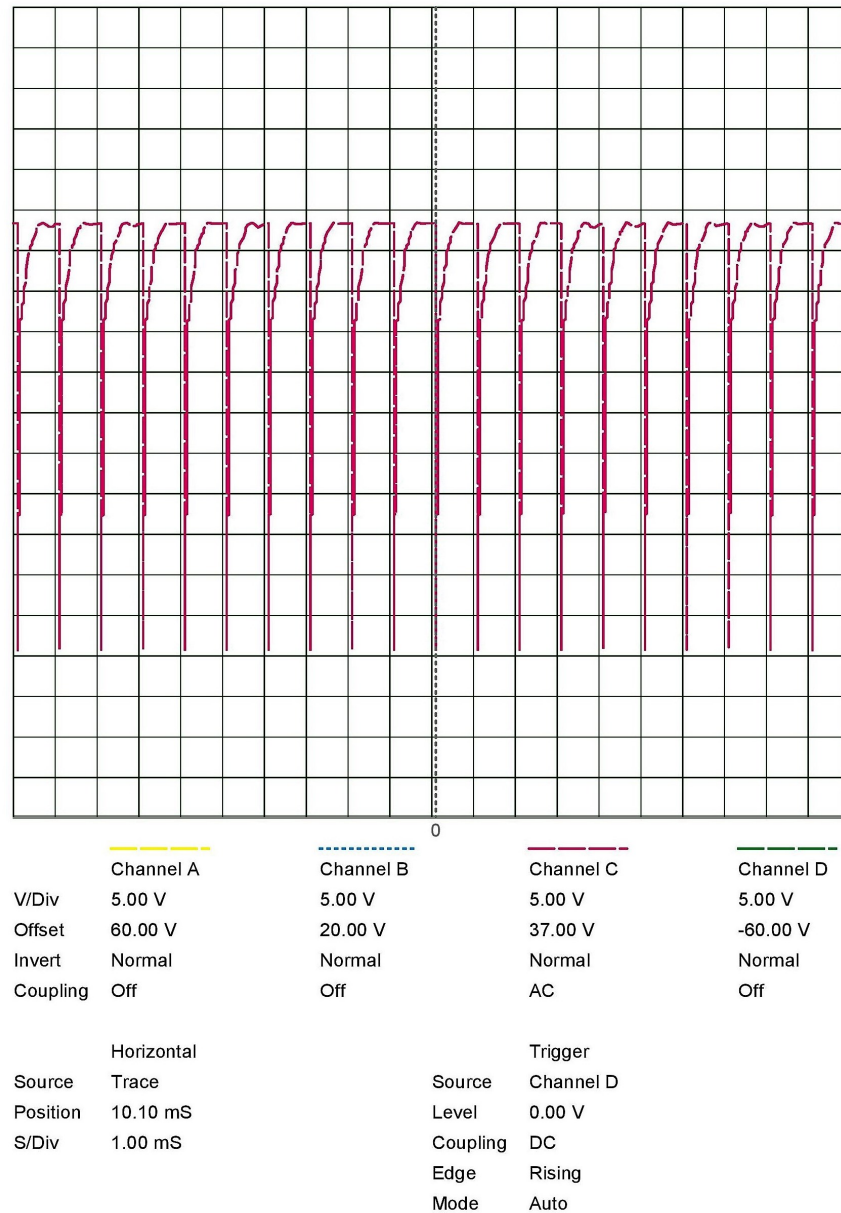


Figure 8. The pulses generated by the modified Marx generator.

The circuits were further analysed for transient responses. In the transient responses' analysis, we chose different values of the capacitors and studied their effect on the output voltage and also on the rise time of the pulses. The transient analysis of the modified Marx generator with optocoupler is shown in Figure 9.

It is clear from Figure 9 that the rise time of the pulse increased linearly as the capacitance value was increased. The output voltage linearly increased until the value of the capacitor was 4 nF and attained the maximum voltage of 49 V; then, it remained constant at a value of 48.7 V. The maximum voltage was limited by the time to charge the capacitor. The rise time linearly increasing with the capacitor was highly undesired. Hence, the circuit was modified (Figure 7) to address the challenge.

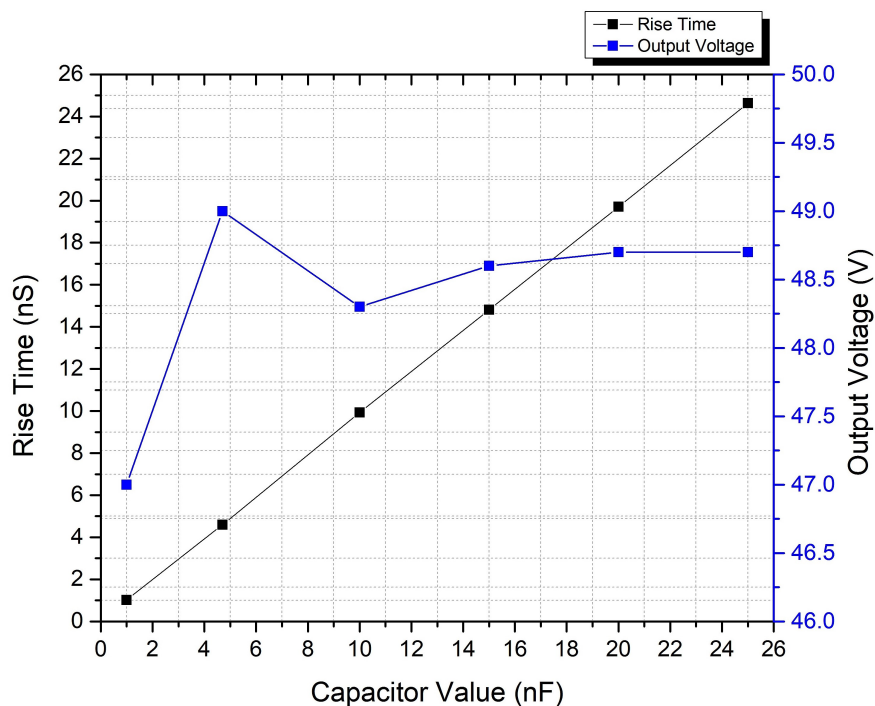


Figure 9. The transient response graph of the modified Marx generator circuit with an optocoupler.

The transient analysis of the modified optocoupler circuit without the optocoupler is shown in Figure 10.

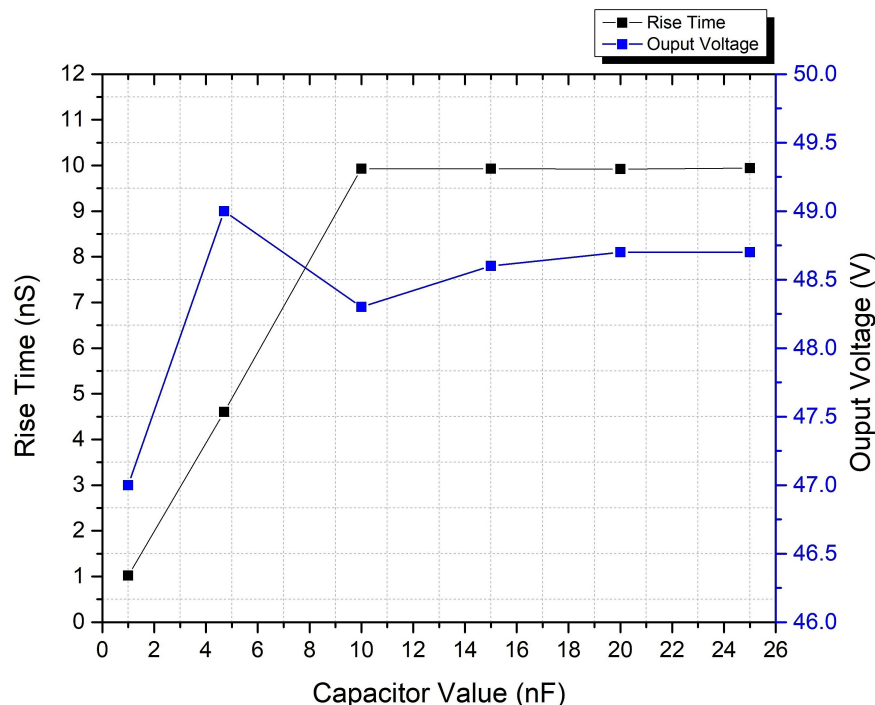


Figure 10. The transient response of the modified Marx generator circuit without the optocoupler.

As shown in Figure 10, the rise time initially increased to a value of 9.93 ns with an increase in the capacitance value, but after that the rise time was constant. It is clear from Figure 10 that the output voltage varied in same manner as it varied in Figure 10. The addition of the optocoupler helps with the fast discharge of the capacitor due to the improved isolation between two parallel capacitors.

The simulated circuit was designed and fabricated in the laboratory for further analysis, as shown in Figure 11.

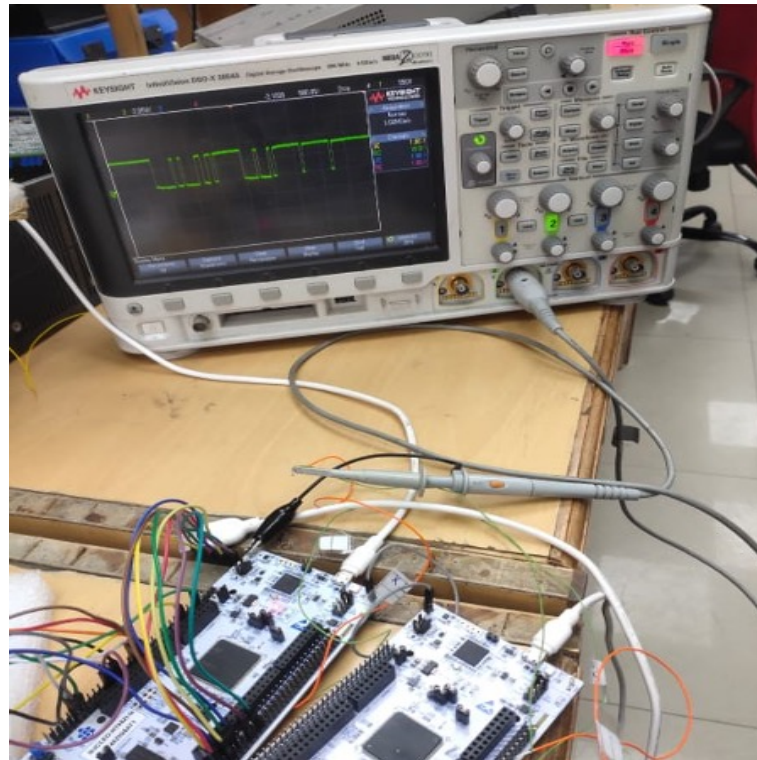


Figure 11. Experimental setup of the proposed pulse generator circuit.

The output voltage waveform as obtained from the oscilloscope (DSO) was exported as a .csv for further plotting of the waveform. The output waveform is shown in Figure 12.

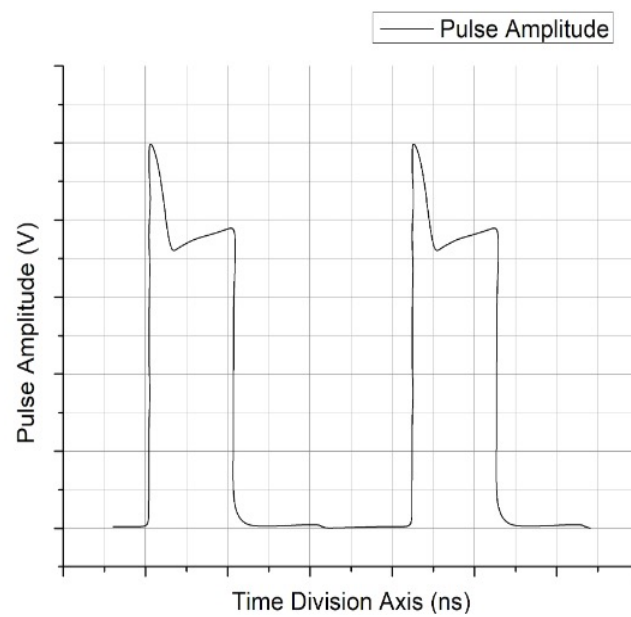


Figure 12. Output voltage waveform obtained from the DSO.

The modified Marx generator presented in this paper was compared with the previously designed Marx generator circuit, as shown in Table 2.

Table 2. Comparison of the previous and proposed modified Marx generator with existing circuits to generate a bipolar pulse.

Ref No.	Number of Stages	Switching Element	Input Voltage	Output Voltage
[45]	12	IGBT	10 kV	120 kV
[46]	2	Spark Gap Switches	50 V	92 V
[18]	4	MOSFET	12 V	30 V
[47]	4	IGBT	12 V	41.2 V
Proposed	5	MOSFET	12 V	49 V

The table shows the different stage Marx generators, input voltage, output voltage, and switching element used in the circuit. As the circuits with an input voltage of 12 V with four stages have a maximum output voltage of 41.2 V, and the proposed circuit has 49 V, it proves that the proposed modified Marx generator achieves the desired boost in the input voltage with minimum components, hence optimizing the size and cost.

4. Conclusions

This paper discussed the challenges of a Marx generator in modern day electroporators.

- One challenge was to achieve bipolar pulses with a minimum number of circuit components.
- Another challenge was the minimization of the pulse shape without minimizing the value of the capacitance, which further decreases the output voltage.

The challenges were addressed in this paper with the modified Marx generator. The modified Marx generator used a power MOSFET as a switch. Further, the optocoupler was used to isolate the parallel capacitors. The optocoupler also served the purpose of switching the MOSFET to bipolar value. The 5-stage MOSFET circuit proposed resulted in 49.4 volts with a 12-volt input. The modified Marx generator rise time of the generated pulses became independent from the capacitor value. Hence, the pulse generated from the modified Marx generator was bipolar and was achieved with a minimum number of components.

Author Contributions: Conceptualization, methodology, S.G., A.T. and D.G.; formal analysis, S.G., D.G., A.T., N.S. and S.R.; software, validation, A.T., S.R., N.S. and A.S., writing—original draft, S.G., D.G., A.T. and N.S.; writing—review and editing, S.R., A.S., D.H.E. and I.D.N.; data curation A.T., A.S., S.R., D.H.E. and I.D.N.; supervision, funding acquisition, A.S., D.H.E. and I.D.N. All authors have read and agreed to the published version of the manuscript.

Funding: The Research was funded by the Princess Nourah bint Abdulrahman University Researchers Supporting Project number (PNURSP2022R238), Princess Nourah bint Abdulrahman University, Riyadh, Saudi Arabia.

Data Availability Statement: Not applicable.

Acknowledgments: Princess Nourah bint Abdulrahman University Researchers Supporting Project number (PNURSP2022R238), Princess Nourah bint Abdulrahman University, Riyadh, Saudi Arabia.

Conflicts of Interest: The authors declare that they have no conflict of interest to report regarding the present study.

References

1. Kotnik, T.; Rems, L.; Tarek, M.; Miklavčič, D. Membrane electroporation and electroporation: Mechanisms and models. *Annu. Rev. Biophys.* **2019**, *48*, 63–91. [[CrossRef](#)] [[PubMed](#)]
2. DeBruin, K.A.; Krassowska, W. Modeling electroporation in a single cell. I. Effects of field strength and rest potential. *Biophys. J.* **1999**, *77*, 1213–1224. [[CrossRef](#)]
3. Yarmush, M.L.; Golberg, A.; Serša, G.; Kotnik, T.; Miklavčič, D. Electroporation-based technologies for medicine: Principles, applications, and challenges. *Annu. Rev. Biomed. Eng.* **2014**, *16*, 295–320. [[CrossRef](#)] [[PubMed](#)]

4. Rubinsky, L.; Guenther, E.; Mikus, P.; Stehling, M.; Rubinsky, B. Electrolytic effects during tissue ablation by electroporation. *Technol. Cancer Res. Treat.* **2016**, *15*, NP95–NP103. [[CrossRef](#)] [[PubMed](#)]
5. Kotnik, T.; Frey, W.; Sack, M.; Meglič, S.H.; Peterka, M.; Miklavčič, D. Electroporation-based applications in biotechnology. *Trends Biotechnol.* **2015**, *33*, 480–488. [[CrossRef](#)] [[PubMed](#)]
6. Zhu, Z.; Zhang, R.; Grimi, N.; Vorobiev, E. Effects of pulsed electric field treatment on compression properties and solutes diffusion behaviors of Jerusalem artichoke. *Molecules* **2019**, *24*, 559. [[CrossRef](#)]
7. Kranjc Brezar, S.; Kranjc, M.; Čemažar, M.; Buček, S.; Serša, G.; Miklavčič, D. Electrotransfer of siRNA to silence enhanced green fluorescent protein in tumor mediated by a high intensity pulsed electromagnetic field. *Vaccines* **2020**, *8*, 49. [[CrossRef](#)]
8. Frandsen, S.K.; Vissing, M.; Gehl, J. A comprehensive review of calcium electroporation—A novel cancer treatment modality. *Cancers* **2020**, *12*, 290. [[CrossRef](#)]
9. Raso, V.H.J.; Heinz, V. *Pulsed Electric Fields Technology for the Food Industry*; Springer: Berlin/Heidelberg, Germany, 2010.
10. Chen, N.; Garner, A.L.; Chen, G.; Jing, Y.; Deng, Y.; Swanson, R.J.; Kolb, J.F.; Beebe, S.J.; Joshi, R.P.; Schoenbach, K.H. Nanosecond electric pulses penetrate the nucleus and enhance speckle formation. *Biochem. Biophys. Res. Commun.* **2007**, *364*, 220–225. [[CrossRef](#)]
11. Kee, S.T.; Gehl, J.; Lee, E.W. *Clinical Aspects of Electroporation*; Springer: New York, NY, USA, 2011.
12. Sharma, A.K.; Debarshi Ghosh, D.; Saluja, N.K.; Singh, T.G. A mathematical model to expedite electroporation based vaccine development for COVID-19. *Bioint. Res. App. Chem.* **2021**, *12*, 1951–1961.
13. Jaeger, H.; Fauster, T.; Schottroff, F. Pulsed Electric Field Process Performance Analysis. In *Pulsed Electric Fields Technology for the Food Industry*; Springer: Berlin/Heidelberg, Germany, 2022; pp. 469–487.
14. Furukawa, T.; Ueno, T.; Matsumura, M.; Amarasiri, M.; Sei, K. Inactivation of antibiotic resistant bacteria and their resistance genes in sewage by applying pulsed electric fields. *J. Hazard. Mater.* **2022**, *424*, 127382. [[CrossRef](#)]
15. Orlacchio, R.; Carr, L.; Palego, C.; Arnaud-Cormos, D.; Leveque, P. High-voltage 10 ns delayed paired or bipolar pulses for in vitro bioelectric experiments. *Bioelectrochemistry* **2021**, *137*, 107648. [[CrossRef](#)]
16. Haldiyan, A.; Ghosh, D.; Saluja, N.; Ganeshan, S.; Singh, T.G. Comparison of Nano-second and Millisecond Pulse Generators for Biological applications of Electroporation. *Res. J. Pharm. Technol.* **2021**, *14*, 2843–2851. [[CrossRef](#)]
17. Elgenedy, M.A.; Darwish, A.; Ahmed, S.; Williams, B.W. A transition arm modular multilevel universal pulse-waveform generator for electroporation applications. *IEEE Trans. Power Electron.* **2017**, *32*, 8979–8991. [[CrossRef](#)]
18. Dwarakanath, S.; Raj, P.; Praveen, K.; Saurabh, S. Generation of HVDC from Voltage Multiplier Using Marx Generator. *Int. J. Adv. Res. Electr. Electron. Instrum. Eng.* **2016**, *5*, 432–4330.
19. Hosseini, S.H.; Saadatizadeh, Z.; Herís, P.C. A new multiport non-isolated bidirectional dc/dc converter with zero voltage switching and free ripple input currents. In Proceedings of the 2017 10th International Conference on Electrical and Electronics Engineering (ELECO), Bursa, Turkiye, 30 November–2 December 2017; pp. 279–284.
20. Liu, S.; Zhang, J.; Zhang, Z. Review of high power compact pulse forming network-Marx generators. *High Power Laser Part. Beams* **2022**, *34*, 075001.
21. Sanders, J.M.; Kuthi, A.; Wu, Y.H.; Vernier, P.T.; Gunderson, M.A. A linear, single-stage, nanosecond pulse generator for delivering intense electric fields to biological loads. *IEEE Trans. Dielectr. Electr. Insul.* **2009**, *16*, 1048–1054. [[CrossRef](#)]
22. Merla, C.; El Amari, S.; Kanaan, M.; Liberti, M.; Apollonio, F.; Arnaud-Cormos, D.; Couderc, V.; Leveque, P. High-Voltage Nanosecond Pulse Generator. *IEEE Trans. Microw. Theory Tech.* **2010**, *58*, 4079–4085.
23. Arnaud-Cormos, D.; Leveque, P.; Wu, Y.H.; Sanders, J.M.; Gunderson, M.A.; Vernier, T. Microchamber setup characterization for nanosecond pulsed electric field exposure. *IEEE Trans. Biomed. Eng.* **2011**, *58*, 1656–1662. [[CrossRef](#)]
24. de Angelis, A.; Kolb, J.F.; Zeni, L.; Schoenbach, K.H. Kilovolt Blumlein pulse generator with variable pulse duration and polarity. *Rev. Sci. Instrum.* **2008**, *79*, 044301. [[CrossRef](#)]
25. Romeo, S.; D’Avino, C.; Zeni, O.; Zeni, L. A Blumlein-type, nanosecond pulse generator with interchangeable transmission lines for bioelectrical applications. *IEEE Trans. Dielectr. Electr. Insul.* **2013**, *20*, 1224–1230. [[CrossRef](#)]
26. Mehta, S.; Puri, V. 7 Level New Modified Cascade H Bridge Multilevel inverter with Modified PWM controlled technique. In Proceedings of the 2021 11th IEEE International Conference on Intelligent Data Acquisition and Advanced Computing Systems: Technology and Applications (IDAACS), Cracow, Poland, 22–25 September 2021; Volume 1, pp. 560–565.
27. Reberšek, M.; Miklavčič, D. Advantages and disadvantages of different concepts of electroporation pulse generation. *Automatika* **2011**, *52*, 12–19. [[CrossRef](#)]
28. Elgenedy, M.A.; Massoud, A.M.; Ahmed, S.; Williams, B.W.; McDonald, J.R. A modular multilevel voltage-boosting Marx pulse-waveform generator for electroporation applications. *IEEE Trans. Power Electron.* **2019**, *34*, 10575–10589. [[CrossRef](#)]
29. Kovalchuk, B.; Kharlov, A.; Kumpyak, E.; Zherlitsyn, A. Pulse generators based on air-insulated linear-transformer-driver stages. *Phys. Rev. Spec.-Top.-Accel. Beams* **2013**, *16*, 050401. [[CrossRef](#)]
30. Jiang, W.; Diao, W.; Wang, X. Marx generator using power mosfets. In Proceedings of the 2009 IEEE Pulsed Power Conference, Washington, DC, USA, 28 June–2 July 2009; pp. 408–410.
31. MacGregor, S.; Tuema, F.; Turnbull, S.; Farish, O. The operation of repetitive high-pressure spark gap switches. *J. Phys. Appl. Phys.* **1993**, *26*, 954. [[CrossRef](#)]
32. Baek, J.W.; Yoo, D.W.; Rim, G.H.; Lai, J.S. Solid state Marx generator using series-connected IGBTs. *IEEE Trans. Plasma Sci.* **2005**, *33*, 1198–1204. [[CrossRef](#)]

33. Sakamoto, T.; Nami, A.; Akiyama, M.; Akiyama, H. A repetitive solid state Marx-type pulsed power generator using multistage switch-capacitor cells. *IEEE Trans. Plasma Sci.* **2012**, *40*, 2316–2321. [[CrossRef](#)]
34. Redondo, L.; Silva, J.F.; Tavares, P.; Margato, E. High-voltage high-frequency Marx-bank type pulse generator using integrated power semiconductor half-bridges. In Proceedings of the 2005 European Conference on Power Electronics and Applications, Dresden, Germany, 11–14 September 2005; p. 8.
35. Sarnago, H.; Burdio, J.M.; Garcia-Sanchez, T.; Mir, L.M.; Alvarez-Gariburo, I.; Lucia, O. GaN-Based Versatile Waveform Generator for Biomedical Applications of Electroporation. *IEEE Access* **2020**, *8*, 97196–97203. [[CrossRef](#)]
36. Darwish, A.; Elgenedy, M.A.; Finney, S.J.; Williams, B.W.; McDonald, J.R. A step-up modular high-voltage pulse generator based on isolated input-parallel/output-series voltage-boosting modules and modular multilevel submodules. *IEEE Trans. Ind. Electron.* **2017**, *66*, 2207–2216. [[CrossRef](#)]
37. Banaei, M.R.; Khiz, A.K. New modular high-voltage pulse generator based on SEPIC converter for electroporation applications. *IET Power Electron.* **2020**, *13*, 3072–3080. [[CrossRef](#)]
38. Davies, I.; Merla, C.; Casciati, A.; Tanori, M.; Zambotti, A.; Mancuso, M.; Bishop, J.; White, M.; Palego, C.; Hancock, C. Push–pull configuration of high-power MOSFETs for generation of nanosecond pulses for electroporation of cells. *Int. J. Microw. Wirel. Technol.* **2019**, *11*, 645–657. [[CrossRef](#)]
39. Achour, Y.; Starzyński, J.; Rąbkowski, J. Modular Marx Generator Based on SiC-MOSFET Generating Adjustable Rectangular Pulses. *Energies* **2021**, *14*, 3492. [[CrossRef](#)]
40. Butkus, P.; Tolvaišienė, S.; Kurčevskis, S. Validation of a SPICE model for high frequency electroporation systems. *Electronics* **2019**, *8*, 710. [[CrossRef](#)]
41. Rodamporn, S.; Beeby, S.; Harris, N.; Brown, A.; Chad, J. Design and construction of a programmable electroporation system for biological applications. In Proceedings of the 1st Symposium Thai Biomedical Engineering, Pathumtani, Thailand, 18–19 December 2007.
42. Redondo, L.; Zahyka, M.; Kandratsyev, A. Solid-state generation of high-frequency burst of bipolar pulses for medical applications. *IEEE Trans. Plasma Sci.* **2019**, *47*, 4091–4095. [[CrossRef](#)]
43. Tarigan, K.; Perangin-Angin, B.; Brahmana, K.; Manalu, A.; Sinambela, M. Simple Designed of High Voltage Pulsed Electric Field Generator Based on Fly-back Transformer. *Physics* **2019**, *1230*, 012027. [[CrossRef](#)]
44. Malviya, D.; Veerachary, M. A Boost Converter-Based High-Voltage Pulsed-Power Supply. *IEEE Trans. Ind. Appl.* **2020**, *56*, 5222–5233. [[CrossRef](#)]
45. Gupta, A.; Mittal, N.; Gurjar, S.; Jalan, S.K.; Talwani, S.; Mehta, S.S. Marx Generator Based High Voltage Using MOSFETs: A Review. *Imp. J. Interdiscip. Res.* **2017**, *3*, 90–94.
46. Chaugule, R.V.; Ruchiharchandani; Bindu, S. Design and hardware implementation of two stage solid state bipolar Marx generator. In Proceedings of the 2016 IEEE International Conference on Recent Trends in Electronics, Information & Communication Technology (RTEICT), Bangalore, India, 17–18 May 2016; pp. 683–687.
47. Saraf, G.; Bansode, A.; Khule, A.; Rangari, S.; Shinde, S. High Voltage Dc Generation using Marx Generator. *IJARCEE* **2017**, *6*, 611–645. [[CrossRef](#)]